Supporting Information

A bidirectional thermal sensory leaky integrate-and-fire (LIF) neuron model based on bipolar NbO_x volatile threshold devices with ultra-low operating current

Jianhui Zhao[1#], Liang Tong[1#], Jiangzhen Niu[1], Ziliang Fang[1], Yifei Pei[2], Zhenyu Zhou[1], Yong Sun[1], Zhongrong Wang[1], Hong Wang[1], Jianzhong Lou[1], Xiaobing Yan[1,2*]

1 *Key Laboratory of Brain-Like Neuromorphic Devices and Systems of Hebei Province, College of Electronic & Information Engineering, Institute of Life Science and Green Development, Hebei University, Baoding 071002, China*

2 *Key Laboratory of Brain-Like Neuromorphic Devices and Systems of Hebei Province, College of Physics Science and Technology, Institute of Life Science and Green Development, Hebei University, Baoding 071002, China*

* *Electronic addresses: xiaobing_yan@126.com, yanxiaobing@ime.ac.cn*

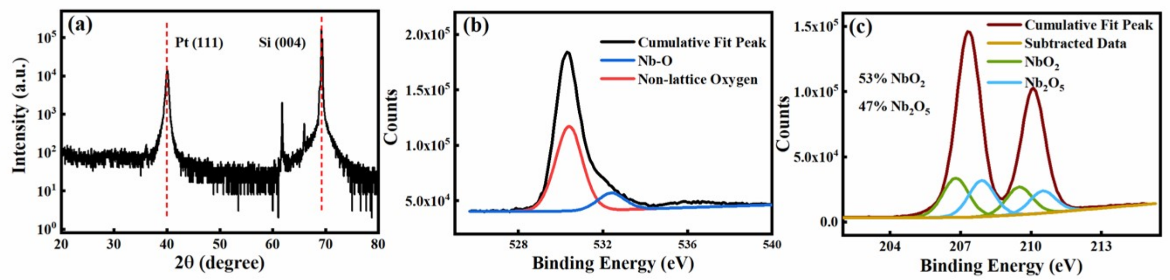

Fig. S1 (a) The X-ray diffraction (XRD) pattern of the prepared amorphous $NbO_x/Pt/Ti/SiO_2/Si$ structure. (b) XPS peaks of O 1s. (c) XPS peaks of Nb 3d.

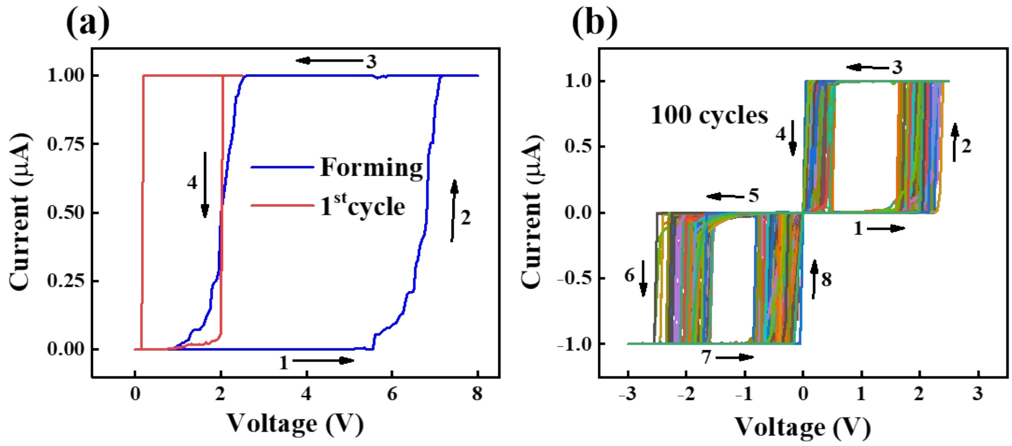

Fig. S2 (a) Electroforming and threshold I-V characteristics of the TiN/NbO_x/Pt device. (b)100 cycles of I-V at 1 μA compliance current.

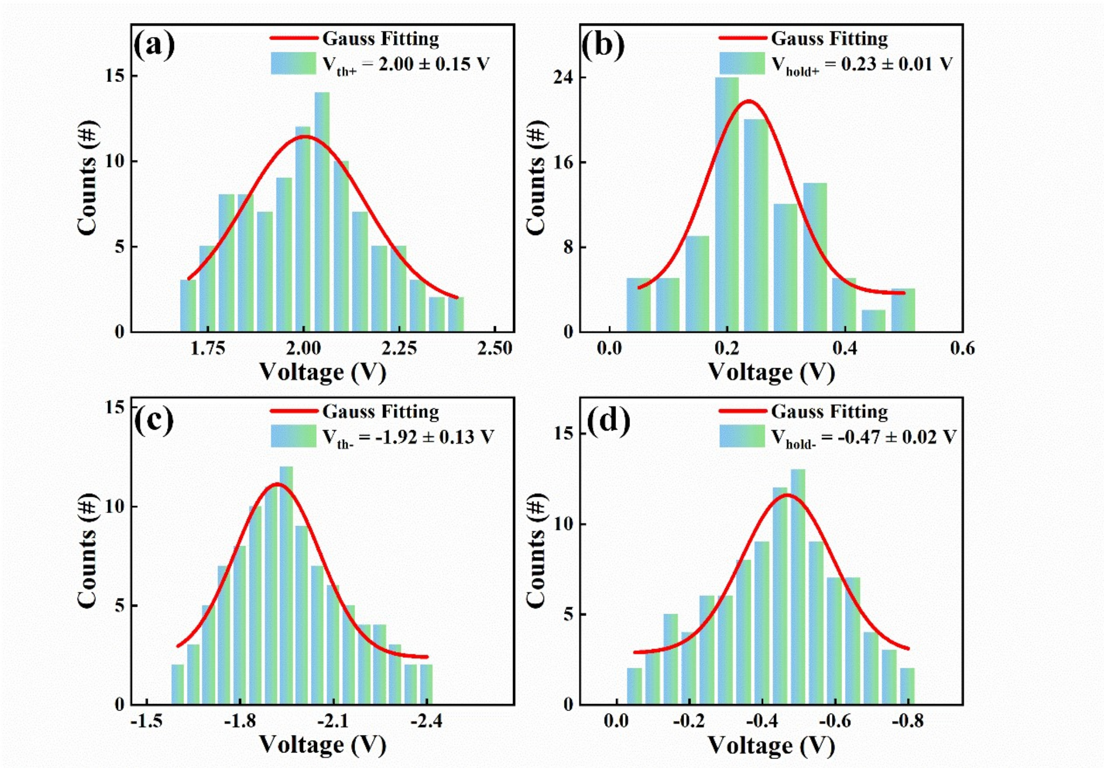

Fig. S3 Statistical chart and Gauss fitting results of (a) V_{th+}, (b) V_{hold+}, (c) V_{th-}, and (d) V_{hold-}.

Table S1. Comparison of off-state current, I_{cc} and I_{ON}/I_{OFF} ratio with other Mott devices.

Material system	Off-state current (A, @1/2 V_{th})	I_{CC}(A)	I_{on}/I_{off} ratio ($I_{CC}/I_{1/2Vth}$)	Reference
Pt/Ti/NbO_x/Pt	~10^{-5}	10^{-4} ~ 10^{-3}	10 ~ 100	[1]
TiN/NbO_x/Si	~10^{-7}	10^{-4}	~1000	[2]
Pd/NbO_x/Pd	~10^{-5}	~8×10^{-4}	~80	[3]
W/NbO_x/W	~2×10^{-6}	10^{-2}	~5000	[4]
Ti/Au/VO_2/Ti/Au	~2×10^{-4}	~2×10^{-2}	~100	[5]
Au/VO_2/Al_2O_3	~0.5×10^{-3}	3.5×10^{-3}	~7	[6]
Pt/VO_2/Pt	~8×10^{-5}	~4×10^{-3}	~50	[7]
Pt/V_3O_5/Pt	~7×10^{-3}	~7×10^{-2}	~10	[8]
TiN/NbO_x/Pt	**~10^{-10}**	**10^{-6}**	**~10^4**	**This work**

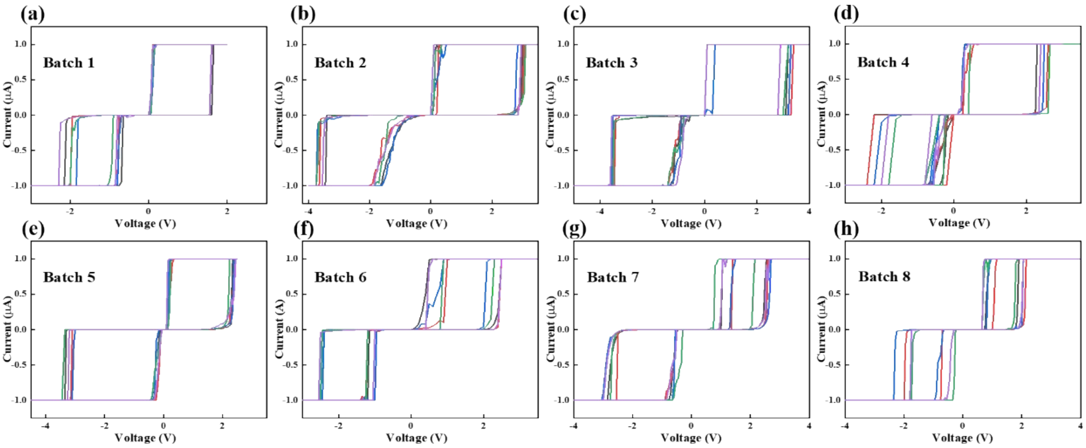

Fig. S4 (a-h) I-V curves for 8 different batches.

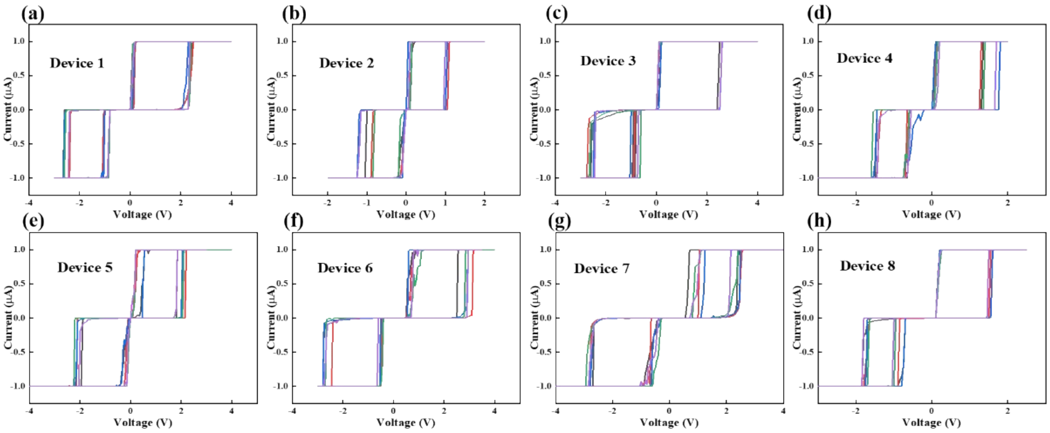

Fig. S5 (a-h) I-V curves for 8 different devices.

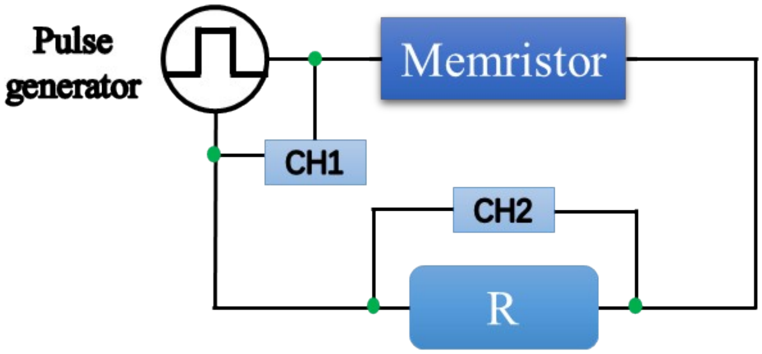

Fig. S6 The test circuit for AC mode.

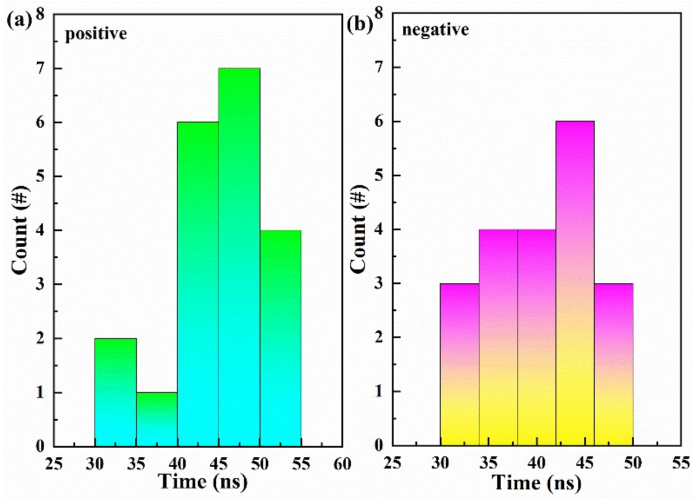

Fig. S7 Statistical distribution of 20 turn-on time at (a) positive voltage, (b) negative voltage.

Table S2. Comparison of switching speeds with other threshold memristors (TSM).

Material system	Turn-on time	Bidirectional or not	Reference
Pt/HfO_2: Ag NDs/Pt	~ 75 ns	×	[9]
Ag/TaO_x/TaO_y/TaO_x/Ag	~ 75 ns	×	[10]
Pd/Ag/HfO_x/Ag/Pd	< 75 ns	×	[11]
Pt/Ti/NbO_x/Pt/Ti	~ 50 ns	×	[12]
Ag/ $Li_4Ti_5O_{12}$/Ag	~ 150 ns	×	[13]
Pt/Ag/SiO_2:Ag/Pt	~ 130 ns	×	[14]
Pt/HfO_2/TiN	~ 80 µs	×	[15]
Ag/WSe_2/Ag	~ 700 ns	×	[16]
TiN/NbO_x/Pt	**Positive: ~44 ns** **Negative: ~40 ns**	✡	**This work**

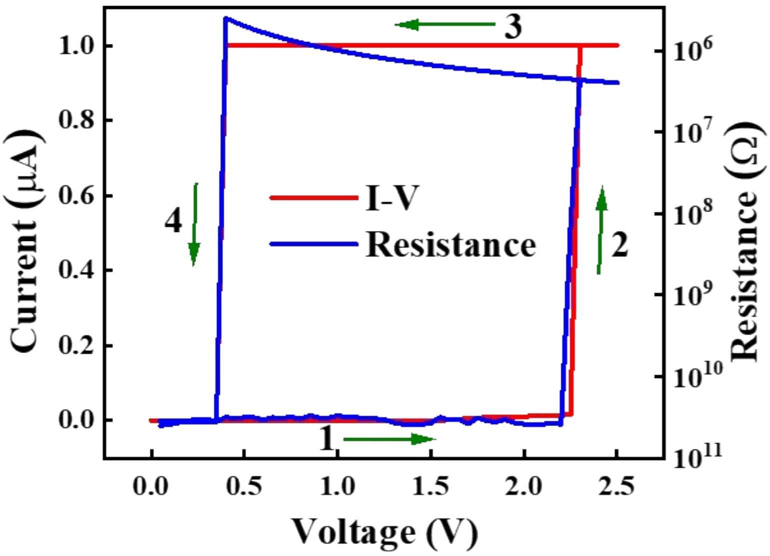

Fig. S8 The I-V characteristics of the device and the corresponding switching of the resistance.

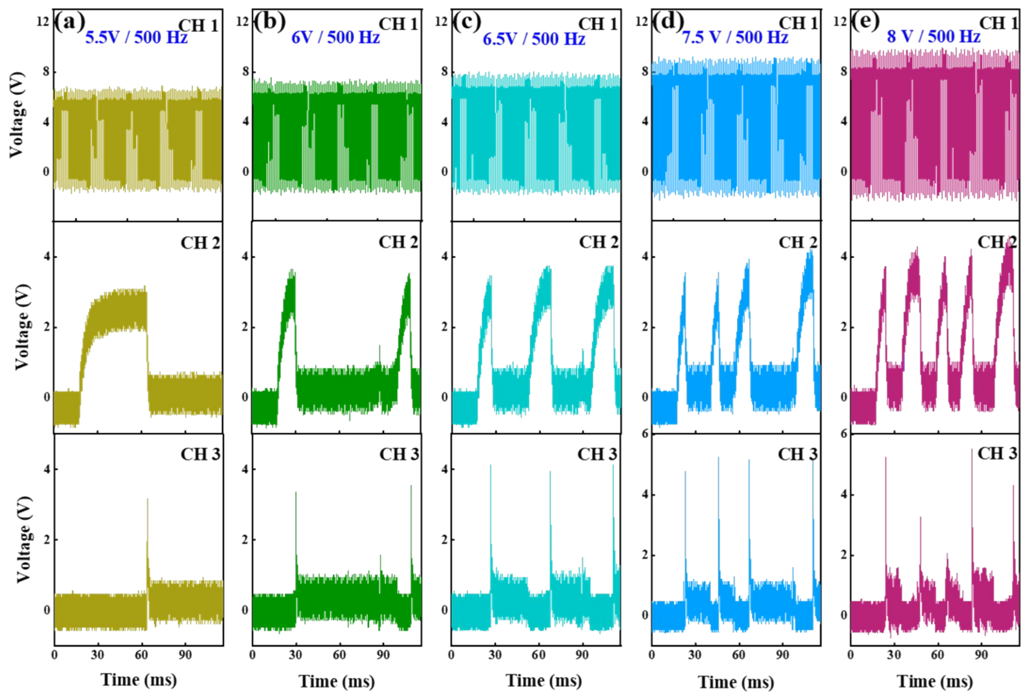

Fig. S9 When R = 5 MΩ, the response of CH1, CH2, CH3. (a) 5.5 V, (b) 6 V, (c) 6.5 V, (d) 7.5 V, (e) 8 V.

Table S3. Comparison with other neuron models.

Material System	Neuron Model	Bidirectional or not	Reference
Ti/Pt/VO_2/Ti/Pt	HH	×	[17]
Pt/NbO_x/Pt	LIF	×	[18]
Pt/Nb_2O_5/Pt	HH	×	[19]
InP/ZnS QDs	LIF	×	[20]
Pt/SiO_xN_y:Ag/Pt	LIF	×	[21]
Pt/TiO_x/Ti	LIF	×	[22]
W/WO_3/PEDOT:PSS/Pt	Quasi-HH	×	[23]
Pt/Ti/NbO_x/Pt/Ti	LIF	×	[12]
TiN/NbO_x/Pt	**LIF**	☼	**This work**

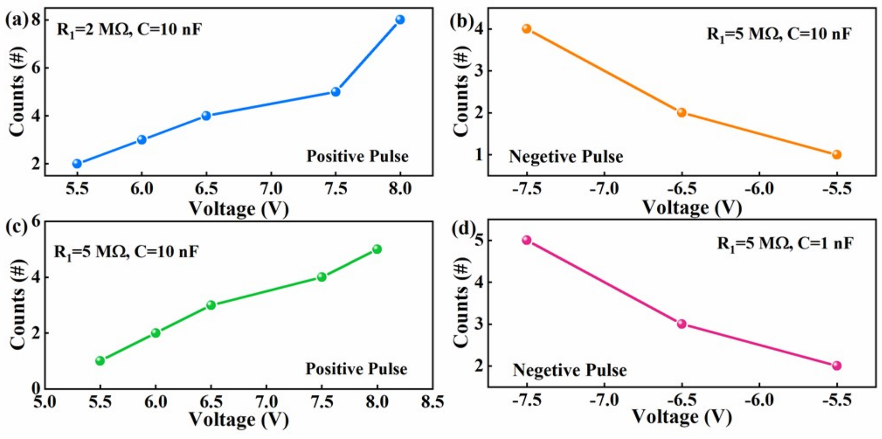

Fig. S10 The number of output spikes at different voltages. (a) R_1= 2 MΩ, (b) R_1= 5 MΩ, (c) C = 10 nF, (d) C = 1 nF.

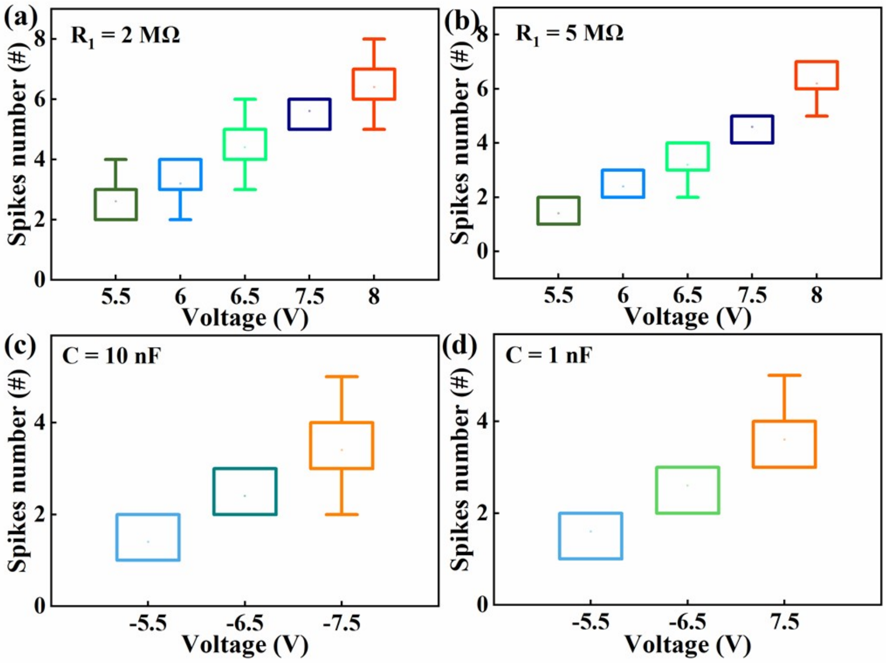

Fig. S11 Statistical box plots of the number of output spikes at different voltages. (a) R_1= 2 MΩ, (b) R_1= 5 MΩ, (c) C = 10 nF, (d) C = 1 nF.

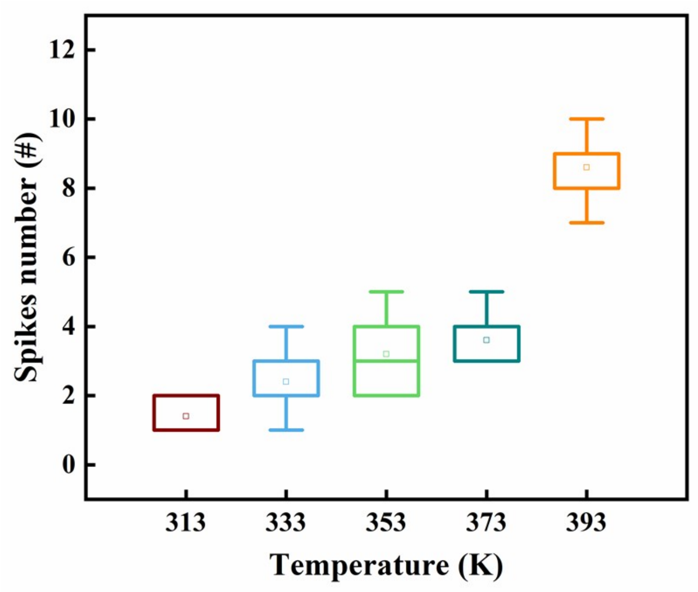

Fig. S12 Boxplot statistics of the spike response of artificial neurons at different temperatures.

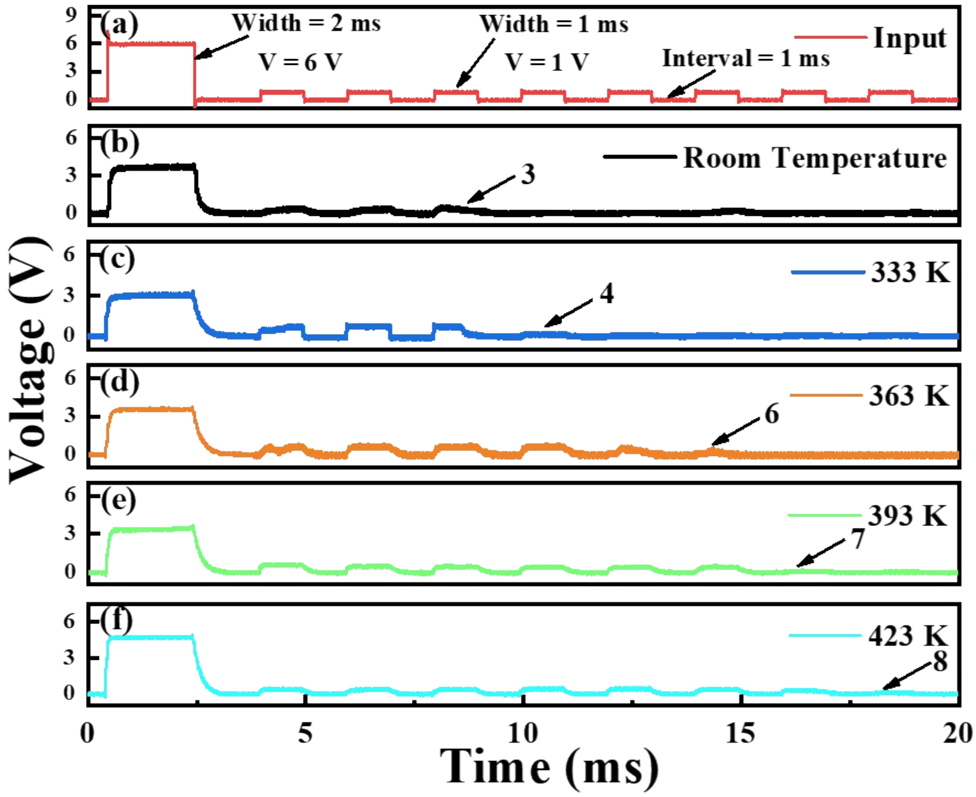

Fig. S13 Turn-off response of the device at different temperatures. (a) Input. (b-f) Room temperature (~293 K), 333 K, 363 K, 393 K and 423 K.

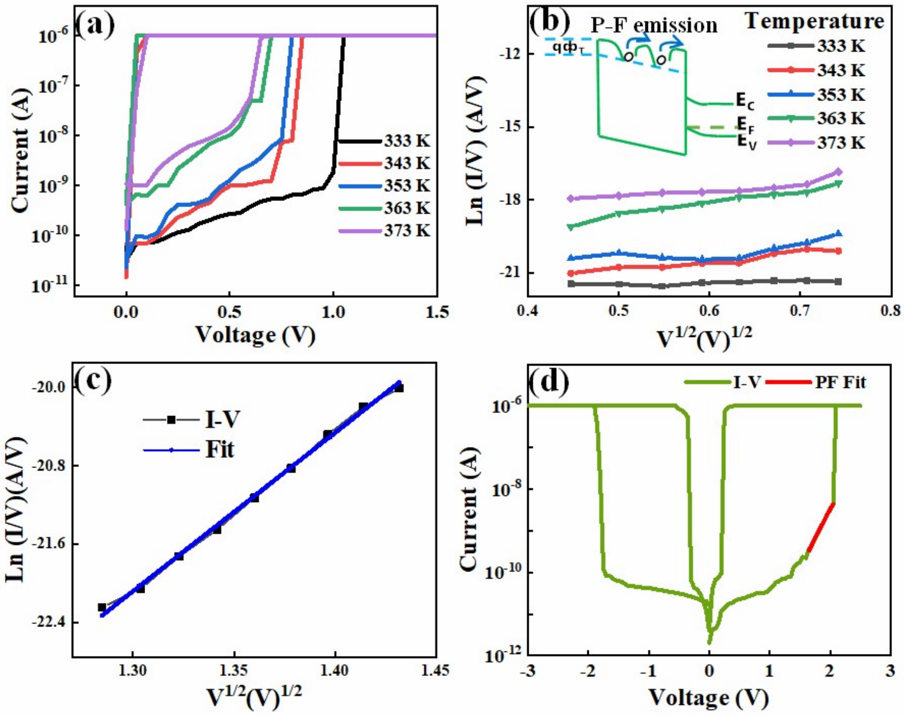

Fig. S14 (a) Logarithmic form of device I-V curve at ambient temperature of 333 K, 343 K, 353 K, 363 K and 373 K. (b) Ln (I/V) vs $V^{1/2}$ plot [Poole-Frenkel (P-F) emission] at different working temperature. (c-d) Fitting curves of P-F emission in the high resistance state of the device.

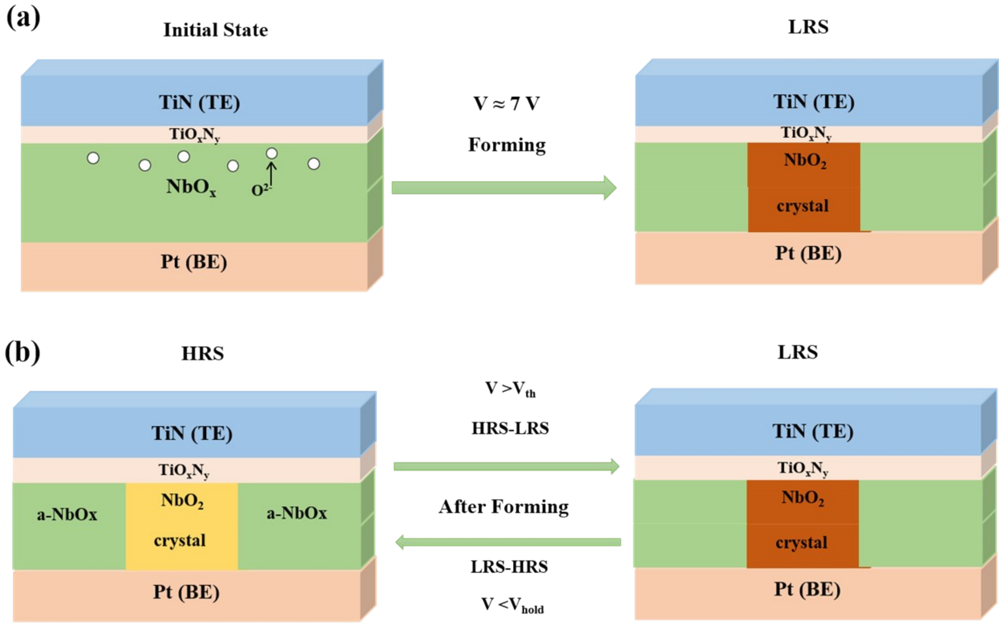

Fig. S15 The schematic of the switching mechanisms. (a) The forming process of the device. (b) The high and low resistance transition of the device after forming.

References

[1] Kim, G. M., *et al.*, *Nat. Commun.* (2021) **12** (1), 8

[2] Zhang, X., *et al.*, *Nat. Commun.* (2020) **11** (1), 51

[3] Li, X., *et al.*, *Adv. Mater.* (2022) **35**, 2203684

[4] Lee, D., *et al.*, *Adv. Electron. Mater.* (2019) **5** (9), 7

[5] Zhou, X., *et al.*, *Adv. Electron. Mater.* (2021) **7** (5), 2001254

[6] Yuan, R., *et al.*, *Nat. Commun.* (2022) **13** (1), 3973

[7] Han, C. Y., *et al.*, *Adv. Mater. Interfaces* (2022) **9** (19), 2200394

[8] Das, S. K., *et al.*, *Adv. Mater.* (2023) **35** (8), 2208477

[9] Li, Y., *et al.*, *Adv. Sci.* (2020) **7** (22), 2002251

[10] Sun, Y., *et al.*, *Adv. Funct. Mater.* (2019) **29** (13), 1808376

[11] Midya, R., *et al.*, *Adv. Mater.* (2017) **29** (12), 1604457

[12] Duan, Q., *et al.*, *Nat Commun* (2020) **11** (1), 3399

[13] Sun, Y., *et al.*, *Adv. Electron. Mater.* (2020) **6** (11), 2000695

[14] Jiang, H., *et al.*, *Nat. Commun.* (2017) **8**, 9

[15] Kim, Y., *et al.*, *Adv. Electron. Mater.* (2019) **5** (7), 1800806

[16] Sivan, M., *et al.*, *Nat. Commun.* (2019) **10**, 12

[17] Yi, W., *et al.*, *Nat. Commun.* (2018) **9**, 10

[18] Zhu, J., *et al.*, *Adv. Mater.* (2022) **34** (24), 2200481

[19] Pickett, M. D., *et al.*, *Nat. Mater.* (2013) **12** (2), 114

[20] Wang, J., *et al.*, *Adv. Funct. Mater.* (2020) **30** (16), 1909114

[21] Wang, Z., *et al.*, *Nat. Electron.* (2018) **1** (2), 137

[22] Park, S.-O., *et al.*, *Nat. Commun.* (2022) **13** (1), 2888

[23] Huang, H. M., *et al.*, *Adv. Mater.* (2019) **31** (3), 8